Ultrafast Dynamics of Polar Monosubstituted Benzene Liquids Studied by the Femtosecond Optical Kerr Effect

Neil A. Smith and Stephen R. Meech*

School of Chemical Sciences, University of East Anglia, Norwich NR4 7TJ, U.K.

Received: September 7, 1999; In Final Form: November 18, 1999

The femtosecond and picosecond dynamics of liquid aniline, nitrobenzene, and benzonitrile have been recorded through measurements of the optically heterodyne detected optical Kerr effect. A major part of the subpicosecond dynamics is assigned to librational motion. This assignment is supported by studies of para-substituted benzonitrile derivatives with differing moments of inertia. The librational frequencies of the three liquids are only weakly dependent on temperature but shift to lower frequency on dilution in inert solvents. The picosecond relaxation dynamics are well described by a biexponential function. The slowest relaxation time behaves, at least qualitatively, as predicted by hydrodynamic models of orientational diffusion. However, quantitative analysis suggests that some of the assumptions concerning the molecular shape or hydrodynamic boundary condition are inadequate to completely describe diffusive orientational motion in these liquids. Measurements of the slowest relaxation time as a function of dilution in nonpolar solvent showed that static orientational pair correlation is negligible in these liquids. The faster of the two picosecond exponential relaxation times could not be ascribed to orientational diffusion, and is instead proposed to arise from structural relaxation occurring on the picosecond time scale in these liquids.

Introduction

Molecular motion in liquids has been studied for many years, using techniques such as depolarized light scattering, Raman scattering, far-IR absorption, and NMR, among others.[1−4] The information gained in these measurements not only aids the understanding of intermolecular forces in the liquid state but also helps in the interpretation of more complex dynamics, such as the dynamics of chemical reactions in solution.[5−8] In some cases, such as in ultrafast electron transfer reactions, the liquid dynamics are thought to be rate controlling,[7−11] in which case a detailed understanding of them is clearly of great importance.

In the past 10 years the technique of femtosecond optically heterodyne detected (OHD) optical Kerr effect (OKE) or, equivalently, Raman induced Kerr effect spectroscopy (RIKES) has come to occupy a prominent place in studies of the dynamics of liquids.[12−40] It has been shown that the femtosecond OHD−OKE experiment is in fact the time domain analogue of Raman spectroscopy and measures the depolarized Raman spectral density.[36,41] Thus, it is intimately related to the depolarized light scattering experiment.[42] However, the data which are obtained in OHD−OKE experiments are of very high quality, especially in the 0−300 cm^{-1} region, which is of most interest for studies of intermolecular dynamics. Further, the experiment has a wide dynamic range, so both ultrafast (<50 fs) and relatively slow (>10 ps) dynamics are measured in the same experiment. The high quality of the data facilitates analysis in terms various models of liquid dynamics.

One area of chemistry where an understanding of liquid dynamics is of particular importance is in the dynamics of solvation. It was suggested some time ago that the ultrafast liquid dynamics, as observed in the OHD−OKE, experiment could be used to model the observation of an ultrafast component in the solvation time correlation function, as measured through time-resolved fluorescence Stokes shift experiments.[43,44] These interesting proposals were given a sound theoretical basis[43−45] and supported by molecular dynamics simulation.[43] The key to a link between the two measurements is that the underlying dynamics of the liquid observed by the two experiments, fluorescence Stokes shift and OHD−OKE, are fundamentally the same. In the case of solvation molecular dynamics simulation suggested that solvent orientational dynamics is the dominant mechanism.[43,46−48] However, polarizability anisotropy relaxation dynamics, as observed in OHD−OKE, are expected to be sensitive to dynamic processes in the liquid which depend on the intermolecular distance (interaction and collision induced dynamics[49,50]) and on local liquid structure (orientational pair correlation[51,52]) in addition to orientational motion.

Early comparisons of measured solvation dynamics with the liquid dynamics recorded through the OHD−OKE experiment were quite encouraging, in that the qualitative features of the solvation dynamics were reproduced.[26,44,53] However, even in these early studies there were some differences in detail between the measured solvation time correlation function and that calculated from the OHD−OKE data.[26,53] More recently a comprehensive comparison of OHD−OKE, dielectric relaxation and solvation dynamics data, for twenty one different liquids, was reported.[54] It was found that the predictions of solvation dynamics based on the OHD−OKE data were markedly inferior to those based on dielectric relaxation measurements.[54] This result suggested that the measurement of polarizability anisotropy relaxation is sensitive to liquid dynamics which are not detected in solvation (or dielectric relaxation) experiments. Since it would appear desirable to be able to translate between all of these different experiments, which all reflect the underlying liquid dynamics, it seems worthwhile to investigate further the nature of the dynamics which contribute to the OHD−OKE measurement.

* Author to whom correspondence may be addressed (e-mail: s.meech@uea.ac.uk)

10.1021/jp993170a CCC: $19.00
Published on Web 01/15/2000

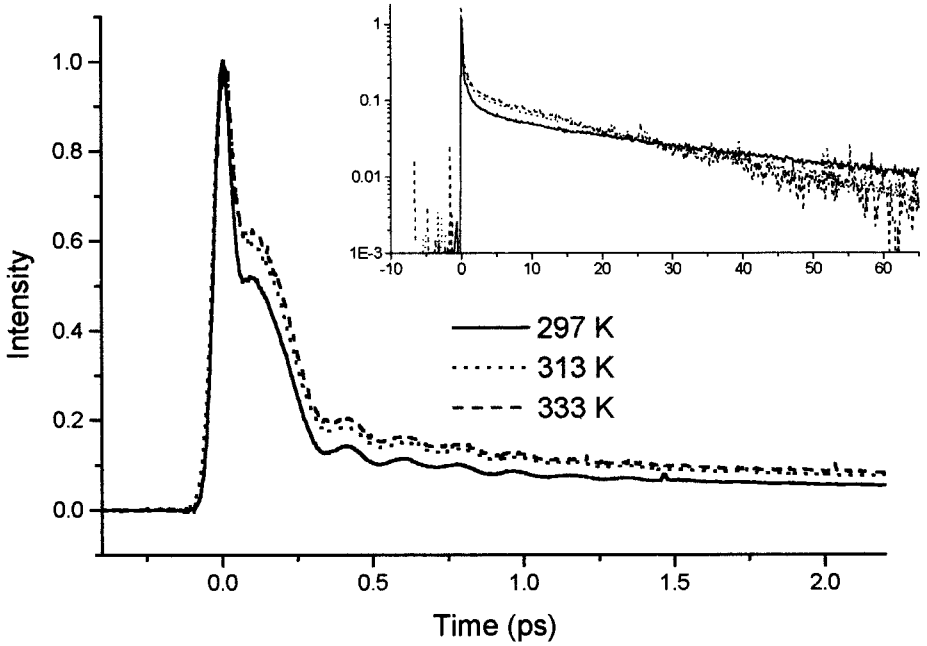

Figure 1. Ultrafast OHD−OKE data for NB measured as a function of temperature at 297 K (solid line), 313 K (dotted line), and 333 K (dashed line). Inset are the data recorded at long times. Note the biexponential form of the latter.

In this article the objective is to look in detail at the OHD−OKE data for three liquids, aniline (AN), benzonitrile (BN), and nitrobenzene (NB), as a function of both temperature and dilution in nonpolar solvents. In addition to these measurements, the dynamics of two para-substituted BN derivatives were also measured, to investigate the effect of varying the moment of inertia. To date the majority of OHD−OKE experiments have been made on neat liquids at a single temperature. This has been the data of most interest for comparison with solvation dynamics and MD simulations. However, there are some fundamental limits on the information which can be extracted from a single OHD−OKE measurement.[55] One approach that has been adopted to overcome this limitation is to compare OHD−OKE data with that from higher order nonlinear optical experiments, which contain additional information.[56−59] For example, the homogeneous and inhomogeneous contribution to the line shape can, in some circumstances, be separated in the fifth order two-dimensional Raman experiment.[57−59] Such a separation is not possible in a single third-order measurement, such as an OHD−OKE experiment. Another approach, the one adopted here, is to study the dynamics of the liquids through the OHD−OKE measurement, but to introduce other variables, such as temperature and dilution. A series of dilution and temperature dependence experiments does contain additional information on the mechanism of the relaxation, the liquid structure, and intermolecular interactions. There are a number of earlier papers in which measurements were made as a function of dilution[20,22,28,32,39] or temperature,[19,40,60−63] or, as here, both.[64]

This paper is organized as follows. In the next section the experimental details and the analysis procedures for the OHD−OKE data are briefly outlined. After that the experimental results are presented. The ultrafast component of the spectral density is analyzed as a function of temperature and dilution. The slowest component of the OHD−OKE relaxation is discussed in terms of diffusive orientational relaxation. In the final section the conclusions of the paper are summarized.

Experimental and Data Analysis

The femtosecond OHD−OKE experiment has been described in great detail elsewhere.[13,22] The current experiments employed a titanium sapphire oscillator which output 300mW in <50 fs transform limited pulses at a frequency of 100 MHz.[25] The OKE setup was of conventional design, and the heterodyne beam was introduced by tilting the input polarizer by 1°, which ensures an out-of-phase local oscillator, so that the signal detected by a diode placed behind the analyzing polarizer, $T(\tau)$, is a convolution of the background free pulse autocorrelation, $G_0^{(2)}(t)$, and the response function of the real part of the third-order susceptibility of the medium, $R_{\text{eff}}(t)$.[65] A typical data set is shown in Figure 1.

The response function of interest can be deconvoluted from the data by taking Fourier transforms of the two measured data sets, $T(\tau)$ and $G_0^{(2)}(t)$, and taking their ratio.[13,16,23,25] To ensure sufficient resolution in the frequency domain, a large number of data points in $T(\tau)$ are required over a wide time range. Typically one trace was recorded with 2.7 fs/datum out to 2 ps, and a second was recorded from 1 to >30 ps with a much larger step size. The latter were fit to a sum of exponentials function (in practice, two exponentials were always sufficient) and the result used to generate a high time resolution data set according to[15]

$$r_s(t) = \left[a_1 \exp\left(-\frac{t}{\tau_1} + a_2 \exp\left(-\frac{t}{\tau_2}\right)\right)\right][1 - \exp(-2\omega_0 t)] \quad (1)$$

where a_1, a_2, τ_1, and τ_2 were recovered from the fit to the data at $t > 1$ ps. The inertial rise of the exponential relaxation is represented by the bracketed term; the choice of ω_0 is not critical.[15] The first, high time resolution data set can then be extrapolated to arbitrarily long times using eq 1, thus ensuring high resolution in the frequency domain data.

The ratio of the two transforms contains the response function, deconvoluted from the effect of the finite pulse width in the frequency domain. The imaginary part of this ratio, the spectral density, $\text{Im}D(\omega)$, contains the information on the nuclear dynamics (the instantaneous electronic response follows the symmetrical shape of the autocorrelation, so does not have an imaginary part). An example of $\text{Im}D(\omega)$ for BN is shown in Figure 2. The same spectral density can also be extracted from the DLS spectrum after correction for a thermal occupation factor.[36]

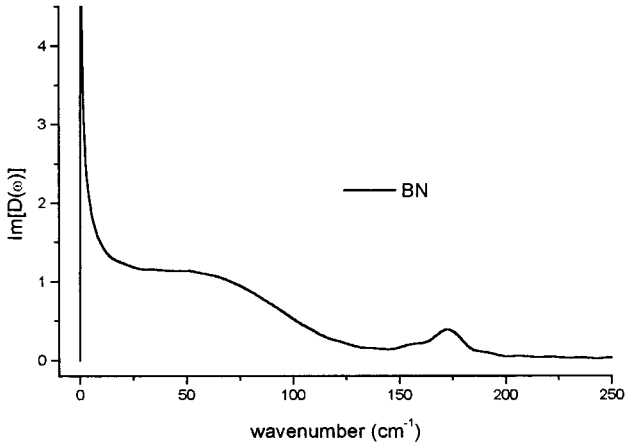

Figure 2. The complete spectral density for BN recovered from the Fourier transform and deconvolution procedure described in the text. The intensity near zero wavenumber arises largely from the components described (in the time domain) by eq 1.

As a starting point for the analysis of the spectral density we, following an established convention,[12−26] treat separately the ultrafast "nondiffusive" and slow "diffusive" (as represented by eq 1) contributions to the dynamics, $R(t) = r_u(t) + r_s(t)$; a test of the desirability of this separation procedure is ultimately one of the objectives of this paper. The separation may be carried out in either the time or frequency domain, with equivalent results.[25] In either case, $r_s(t)$ [or $r_s(\omega)$] is subtracted from $R(t)$ [or Im$D(\omega)$]. The resultant line shapes for all three liquids at 297 K are shown in Figure 3. Also discernible in Figure 3 are slight oscillations in the data at low frequency. These arise from an imperfect match between the short and the long time data. For each liquid the ultrafast part of Im$D(\omega)$ is shown fit to a sum of two functions,[22−24] an antisymmetrized Gaussian

$$I_G(\omega) = g_1 \exp\left[\frac{-2(\omega - \omega_1)^2}{\Delta\omega^2[2\ln(2)]^{-1}}\right] - g_1 \exp\left[\frac{-2(\omega + \omega_1)^2}{\Delta\omega^2[2\ln(2)]^{-1}}\right] \quad (2)$$

and the generalized ohmic line shape

$$I_{BL}(\omega) = b\omega^{\alpha} \exp\left(-\frac{\omega}{\omega_{BL}}\right) \quad (3)$$

In general eq 2 is taken to represent an inhomogeneously broadened librational mode of the liquid, frequency ω_1. Equation 3 was derived for a purely collision induced line shape (by Bucaro and Litovitz, hence BL) in atomic and molecular liquids, in this case specific values of α result.[50] However, the more general ohmic line shape ($\alpha = 1$) is found to describe a variety of relaxation phenomena.[66]

In addition to fitting the ultrafast Im$D(\omega)$ to these line shapes we also attempted to describe them in terms of a sum of two Brownian oscillators[19,55]

$$\mathrm{Im}D(\omega) = \sum_i \frac{\omega\eta_i\kappa_i}{2\pi[(\omega_i^2 - \omega^2)^2 + \omega^2\gamma^2]} \quad i = 1, 2 \quad (4)$$

an approach which has been successful in describing Im$D(\omega)$ for acetonitrile.[67] In eq 4 ω_i is the frequency of the ith mode, κ_i is the coupling strength, and γ_i is the damping (the friction induced by the heat bath on the ith oscillator). In eq 4 γ_i has been assumed frequency independent.[19,55] The fit of eq 4 is seen to be acceptable for AN and NB, but less good for BN (Figure 4). In general eq 4 with $i = 2$ gives a much less good fit than eq 2 + eq 3. The main failure of the Brownian oscillator analysis is on the high frequency side of the spectral density, where it may be seen that the function does not return to the baseline as quickly as the data. The fit is not therefore improved by adding a third oscillator, although we note that Bartolini et al. were able to describe accurately the spectral density of iodobenzene with a sum of five Brownian oscillators.[40] An attempt was also made to fit the data of Figure 3 to a sum of two Gaussians, representing two inhomogeneously broadened oscillators (or two distinct degrees of freedom) in the librational spectrum. This

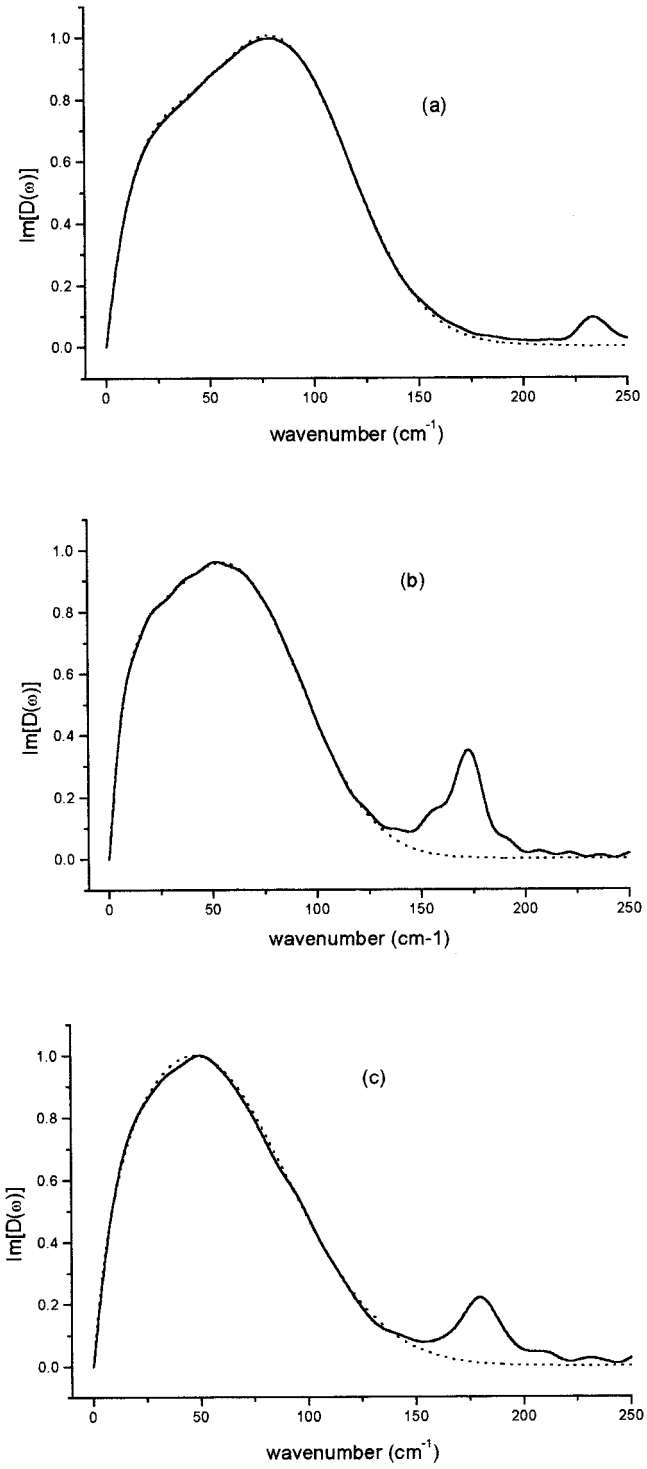

Figure 3. The ultrafast spectral density (i.e., the component fit by eq 1 has been subtracted) at 297 K for (a) AN, (b) BN, and (c) NB (solid lines). The spectral densities have been fit to eq 2 + eq 3 (dotted lines).

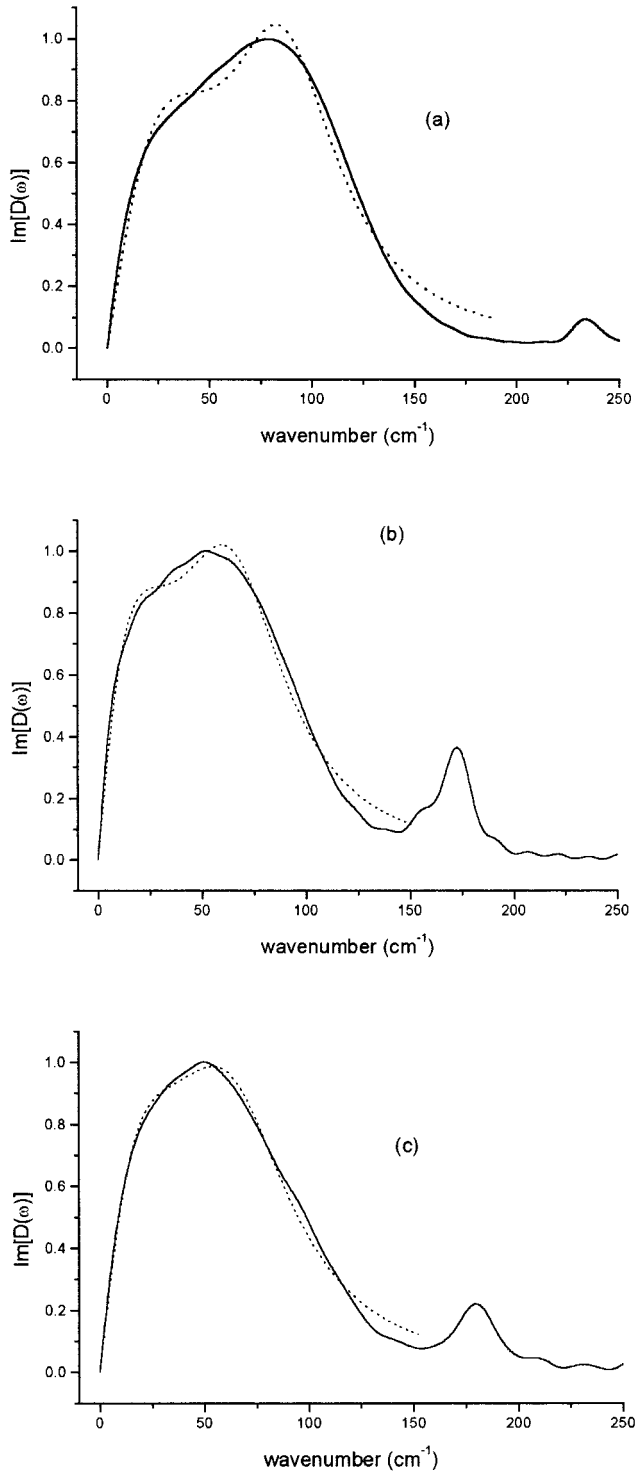

Figure 4. As Figure 3, but the data are fit to two Brownian oscillators, eq 4. Note the relatively poor fit compared to Figure 3, especially at higher frequency.

approach was successful in Friedman and She's study of iodobenzene.[68] In all of the liquids studied here, this fit was less satisfactory even than that of the two Brownian oscillators and will not be considered further.

The analysis of the long, exponential relaxation components was initially based on the assumptions of hydrodynamic models of diffusive reorientation, for which the viscosity is required. Viscosity was measured using a calibrated capillary viscometer contained in a thermostated water bath. The results were checked against the previously reported values for the pure liquids.[69]

All samples were used as received, except for the AN, which had a slight yellow color. AN was distilled under reduced pressure until clear. (It was found that this purification did not in fact alter the observed dynamics.) The samples were injected into the 2 mm path length silica sample cell through a 2 μm filter to remove any solid particles, and so reduce scattered light. For the measurements of the OHD−OKE data as a function of temperature, the sample cell was placed in a thermostated copper block through which heated oil was flowed. The substituted BN derivatives were hot filtered directly into the sample cell and melted in the thermostated sample holder.

The effective moments of inertia, $I_{\text{eff}}^{-1} = I_{xx}^{-1} + I_{yy}^{-1}$, were required for some analyses, and these were obtained from calculations using the commercial Hyperchem calculation package.

3. Results and Discussion

3.1. Ultrafast Spectral Density. We have recorded the ultrafast Im$D(\omega)$ for the three pure liquids as a function of temperature, and for BN and NB as a function of dilution, in heptane, isopentane, and CCl_4. AN was also studied as a function of dilution in CCl_4, the only nonpolar solvent with which it was miscible. However, the ultrafast spectral densities obtained in CCl_4 are ambiguous because of the necessity of subtracting from the data the response of CCl_4 itself, which is appreciable. This can be done by subtracting the spectral density of pure CCl_4 from the response of the mixture. The size of the CCl_4 contribution can be estimated by normalizing with respect to the intensity of the CCl_4 intramolecular modes at 218 and 314 cm^{-1}.[70] However, this assumes that the shape of the intermolecular spectral density is independent of dilution. Since the CCl_4 spectral density is largely collision induced this assumption does not seem justified (unless the CCl_4 volume fraction is large). For this reason the Im $D(\omega)$ recorded on dilution of the liquids in CCl_4 will not be described further, although they showed qualitatively the same trends as were observed in the alkane solvents.

The data for the remaining samples are presented in Table 1. They have been fit to either a sum of eqs 2 and 3 or to eq 4. We note again that the fit to eq 4 is of lower quality (see Figures 3 and 4). To illustrate the behavior observed the temperature dependence of Im $D(\omega)$ for BN and AN is shown in Figure 5, and the dilution dependence for NB and BN in Figure 6. The fact that the fit to eq 2 + eq 3 is so successful should not be taken to imply that there are necessarily two distinct, separable, dynamical processes contributing to the ultrafast Im $D(\omega)$ line shape; rather, it shows that these liquids (and the 20 or so others where a fit to these two functions is successful[21−26,30−32,54]) have a quite general line shape. The particular features of this common line shape are an antisymmetrized Gaussian peaked between 40 and 70 cm^{-1} which is broadened and acquires extra intensity on the low frequency side, this broadening being rather well represented by eq 3.

The spectral densities of AN and BN are shown in Figure 5 as a function of temperature. The result for NB was very similar. The effect of an increase in temperature can be seen from Figure 5 to be small, being a slight decrease in the width of the spectral density, accompanied by a shift to lower frequency. A similar form of temperature dependence was noted by Fourkas and coworkers in their study of acetonitrile and CS_2.[62] These trends are not brought out strongly in the fitting parameters (Table 1), probably because the size of the shift is smaller than the error in the fitting. (It should be noted that there is considerable "cross talk" between the fitting functions eq 2 and eq 3, such that small changes in one can be compensated for by changes in the other,

TABLE 1: Numerical Data for Some of the Ultrafast Spectral Densities Measured[a]

			eq 2 + eq 3					eq 4						eq 1	
sample	temp	comp.	a_1	ω_{BL}	a_2	ω_1	$\Delta\omega$	a_1	ω_1	γ_1	a_2	ω_2	γ_2	τ_1	τ_2
AN	297 K		0.08	30	0.92	88	71	0.3	48	91	0.70	91	66	1.5	16.8
	333 K		0.07	24	0.93	82	77	0.3	45	86	0.70	88	65	1.0	7.3
	353 K		0.07	27	0.93	80	77	0.34	48	83	0.66	89	63	nm	nm
BN	297 K		0.09	14	0.91	61	79	0.27	36	78	0.73	72	66	1.8	19.9
	333 K		0.08	18	0.92	61	74	0.33	38	74	0.67	71	60	1.2	11.8
	353 K		0.09	13	0.91	56	79	0.29	35	73	0.71	69	63	1.1	8.9
NB	297 K		0.05	14	0.95	46	103	0.25	38	76	0.75	72	76	1.9	34.7
	333 K		0.06	15	0.94	51	86	0.28	36	69	0.72	67	66	1.5	21.3
	353 K		0.07	20	0.93	51	88	0.36	38	69	0.64	69	64	1.4	17.1
BN/hept		10%	0.08	11	0.92	37	77	0.36	32	62	0.64	57	53	0.5	4.3
		50%	0.11	14	0.89	55	73	0.32	33	71	0.68	65	61	1.7	12.5
		75%	0.07	24	0.93	59	71	0.41	41	71	0.59	70	57	1.5	13.9
NB/hept		10%	0.08	23	0.90	30	83	0.50	34	56	0.50	62	55	1.1	7.3
		50%	0.10	16	0.91	42	92	0.34	35	73	0.66	64	71	2.1	16.3
		75%	0.06	15	0.94	41	98	0.28	34	68	0.72	66	70	1.6	20.1
BN/iso		10%	0.11	12	0.89	40	75	0.40	29	60	0.60	56	55	1.1	4.6
		50%	0.10	15	0.90	56	74	0.31	35	75	0.69	67	63	1.4	11.1
		75%	0.10	14	0.90	59	77	0.28	35	81	0.72	70	69	2.0	16.0

[a] Data are fit to the line shape functions described in the text. All frequencies and damping constants given in wavenumbers. Also included for later reference are the numerical values of the relaxation times in picoseconds measured by fitting the long time data to eq 1 (accuracy ± 10% except for the short relaxation times in the dilution experiments, where ± 0.5 ps is more realistic).

to yield a fit of very similar quality.) The BO fits do show the shift to low energy in the higher frequency component, but the quality of the fit is relatively poor. It may also be noted that the damping constant remains the same or decreases with increasing temperature (Table 1). A decrease is unexpected, and suggests that not too much physical significance can be ascribed to these fitting parameters.

The main result from Figure 5 is that the spectral density is only weakly dependent on temperature. This result can be understood if the antisymmetrized Gaussian, which is the dominant component in the fit (Table 1) is modeled in terms of an orientational−librational mode of the liquid. The librational motion is assumed to take place on a harmonic potential surface arising from interactions of the molecule with a surrounding cage of nearest neighbors.[71] The width of the Gaussian is, in the inhomogeneous limit, derived from a distribution of librational frequencies due to a distribution of cage structures. This is clearly an oversimplification; in reality each librational oscillator will also have associated with it a finite homogeneous width. Since the librational frequency depends on the intermolecular interactions, dipole−dipole, dipole−induced dipole, etc., and these are not strongly temperature dependent, the slight temperature dependence in Figure 5 is consistent with the librational model. The small shift to lower frequency might be explained by a decreasing density with increasing temperature, leading to weaker intermolecular interactions, because of the on average larger intermolecular distance. It should be noted, however, that a weak temperature dependence would also be expected for some other contributions of the intermolecular dynamics to the line shape, for example the collision induced dynamics represented by eq 3.

To investigate whether the assignment of the antisymmetrized Gaussian to a librational mode of the liquid is reasonable we have measured Im$D(\omega)$ for *p*-tolunitrile and *p*-fluorobenzonitrile. The data are shown in Figure 7 and Table 2. Clearly the derivatives with higher moments of inertia have spectral densities which are shifted to lower frequencies than pure BN. If we assume that the librational frequency is given by $(k/I_{eff})^{1/2}$, where k is the force constant of the harmonic potential surface, then the shift observed is in the expected direction. If the further approximations that k is determined only by intermolecular interactions and that these interactions are similar for the three derivatives (BN and its *p*-fluoro derivative at least have similar boiling points) are made, then $(\omega_{1,BN}/\omega_1) = (I_{eff}/I_{eff,BN})^{1/2}$ is expected. The results of this calculation are also shown in Table 2, and it can be seen that the agreement is reasonable, given the approximations involved. These results provide supporting evidence for the assignment of the main high frequency part of the ultrafast spectral density of these liquids to librational dynamics. In contrast if the molecular mass, rather than the moment of inertia, were the important parameter, as might be the case for a collision induced contribution to the line shape, the spectral shifts predicted for the substituted BN are smaller than those observed.

The spectral densities of BN and NB as a function of dilution in nonpolar solvents are shown in Figure 6. In both cases the traces narrow and the peak frequencies shift to lower energy with increasing dilution. The fitted data are given in Table 1 and reflect these trends. The table also shows that the antisymmetrized Gaussian remains the dominant constituent of the spectral density, the ohmic line shape accounting for only about 10% of the whole. The origin of these shifts can be readily understood in terms of the "librational motion in a cage" model described above. As the mole fraction of the non polar weakly polarizable constituent of the mixture increases it will make up a larger portion of the cage. Since the force constant depends on the strength of the intermolecular interaction, the librational frequency is expected to decrease with increasing dilution, as observed. A similar explanation was given for the shifts observed for Im$D(\omega)$ of CS_2 in pentane.[20]

Two alternative explanations have been offered for spectral shifts on dilution. First, as the polar polarizable molecules are diluted in the nonpolar solvent it is expected that the collision and interaction induced contributions to Im$D(\omega)$ will also be progressively reduced.[39] This will have the effect seen in Figure 6 if these contributions are largely responsible for the high frequency (above 50 cm^{-1}) part of the spectral density. This possibility cannot definitely be excluded on the basis of the present data. However, the study of the spectral density as a function of I_{eff} for derivatives of BN (above) suggested a librational origin for the higher frequency component. Further, MD simulations on simpler molecules, such as acetonitrile,

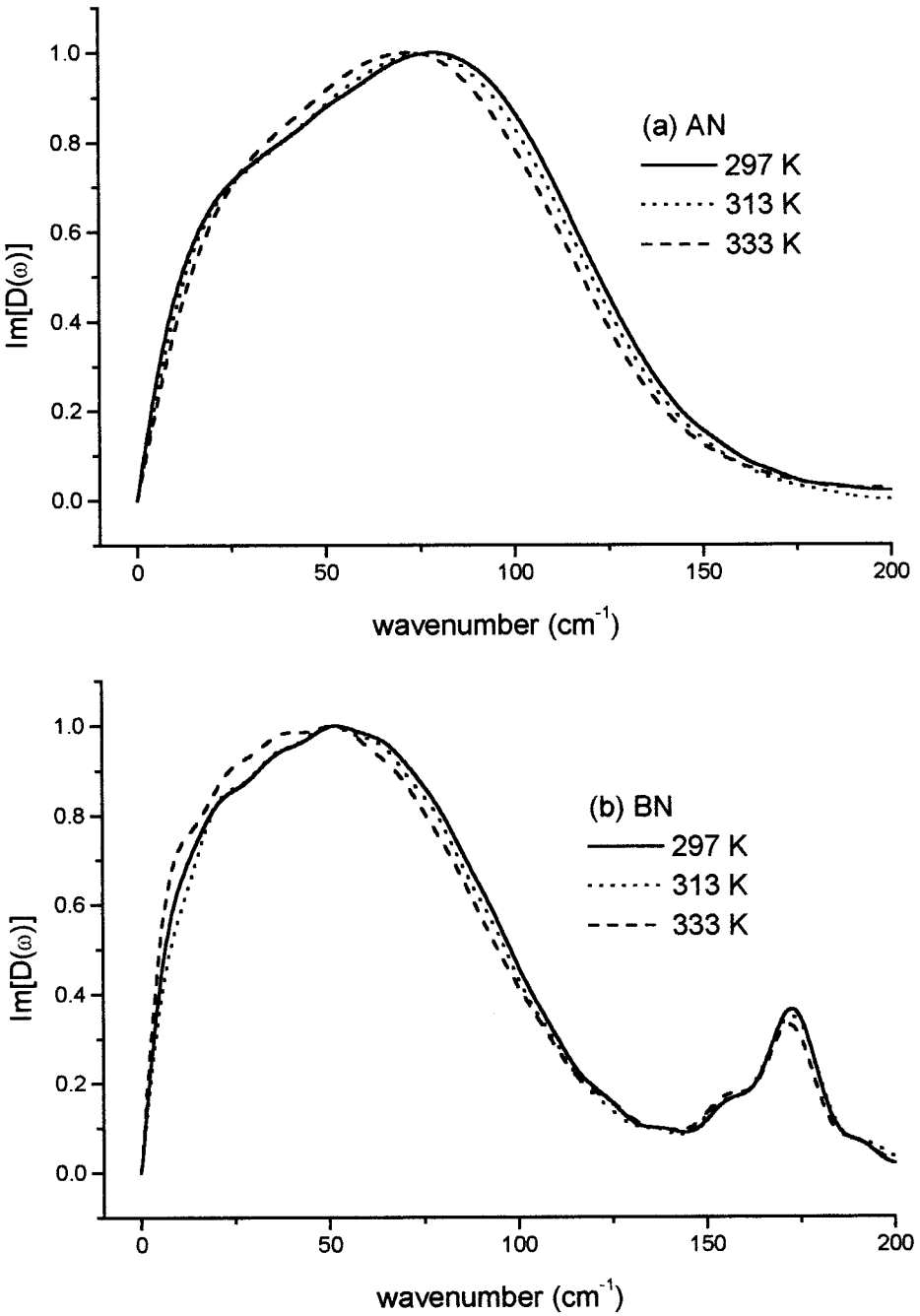

Figure 5. The temperature dependence of the spectral densities for (a) AN (b) BN measured at 297 K (solid line), 313 K (dotted line), 333 K (dashed line).

suggest that interaction induced components of the relaxation of the polarizability anisotropy contribute over a wide range of time scales, and not just at ultrafast times (high frequency).[49,72]

A second effect that could occur on dilution is the disruption of specific dimeric structures in the liquid[15,32] to form monomers.[70] If the intermolecular dimer mode was at high frequency and the monomer librational mode at lower frequency then this might account for the shifts observed in Figure 6. Although we have not found any data from gas-phase spectroscopy on BN and NB dimers, those that have been reported for other benzene derivatives have some modes at around 10−50 cm^{-1}.[73,74] Thus elimination of a dimer mode on dilution is a plausible explanation for the observations of Figure 6. However, it is noted that the shift on dilution is continuous, and that the spectral density is nearly temperature independent, neither of which are necessarily expected for a simple monomer−dimer equilibrium.

3.2. Picosecond Orientational Relaxation. In this section the slower relaxation dynamics, which were fit to eq 1, will be analyzed in terms of the small step diffusion model developed by Debye[75] and described in detail many times in the intervening years.[42,64,76−79] In the OHD−OKE experiment the molecular reorientation is monitored through the polarizability anisotropy relaxation. If it is assumed that the polarizability tensor and diffusion tensor of the molecules considered here share a common axis system then the OHD−OKE data are expected to relax as a sum of two exponential terms[42,64]

$$r_{OR}(t) = \frac{A_1}{\tau_{r1}} \exp(-t/\tau_{r1}) + \frac{A_2}{\tau_{r2}} \exp(-t/\tau_{r2}) \qquad (5a)$$

This result is at least qualitatively consistent with the result noted

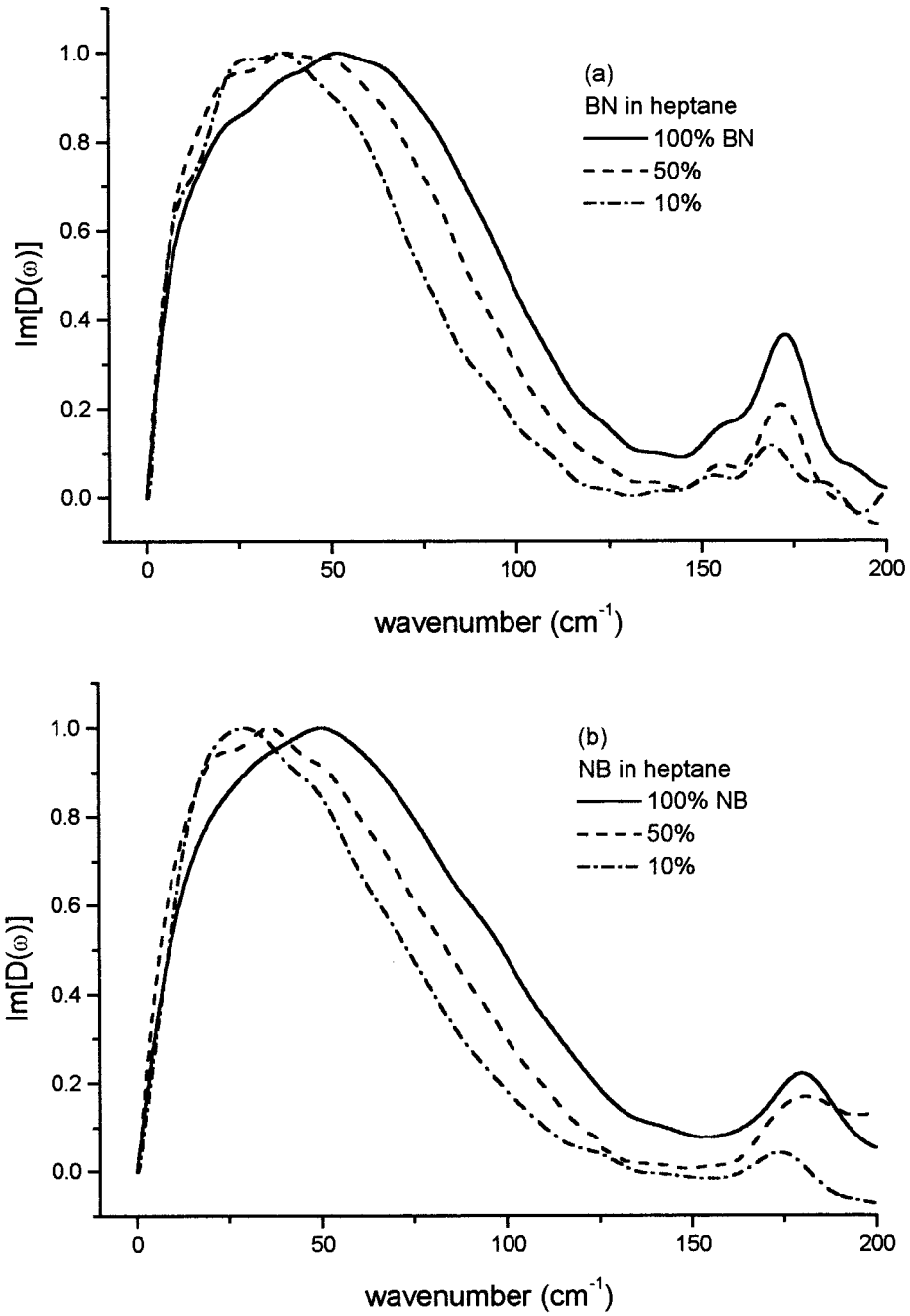

Figure 6. Spectral densities for (a) BN and (b) NB at various volume fractions in heptane.

above, that the slow relaxation is always observed to be biexponential. In eq 5a

$$\tau_{r1} = \frac{1}{6\Theta_I + 2\Delta} \quad \tau_{r2} = \frac{1}{6\Theta_I - 2\Delta} \tag{5b}$$

and

$$\Theta_I = (\Theta_{xx} + \Theta_{yy} + \Theta_{zz})/3 \tag{5c}$$

$$\Delta = [(\Theta_{xx} - \Theta_{yy})^2 + (\Theta_{zz} - \Theta_{xx})(\Theta_{zz} - \Theta_{yy})]^{1/2} \tag{5d}$$

$$A_1 = \frac{1}{N^2}\left(\frac{a^2\alpha_1^2}{3} + \frac{ab\alpha_1\alpha_2}{\sqrt{3}} + \frac{b^2\alpha_2^2}{2}\right) \tag{5e}$$

in which

$$\alpha_1 = \alpha_{zz} - 0.5(\alpha_{xx} + \alpha_{yy})$$
$$\alpha_2 = \alpha_{xx} - \alpha_{yy}$$
$$a = \sqrt{3}(\Theta_{xx} - \Theta_{yy}) \tag{5f}$$
$$b = 2\Theta_{zz} - \Theta_{xx} - \Theta_{yy} + 2\Delta$$
$$N = 2(\Delta b)^{1/2}$$

and the α_{ii} are the elements of the polarizability tensor. A_2 has the same form as A_1 but a and b are interchanged and a minus sign precedes the second term. The unknowns in eqs 5 are the diffusion coefficients, Θ_{ii}, which are given in the modified Debye theory by

$$\Theta_{ii} = kT/\eta\lambda_i V \tag{6}$$

which can, in the hydrodynamic limit, be determined from a

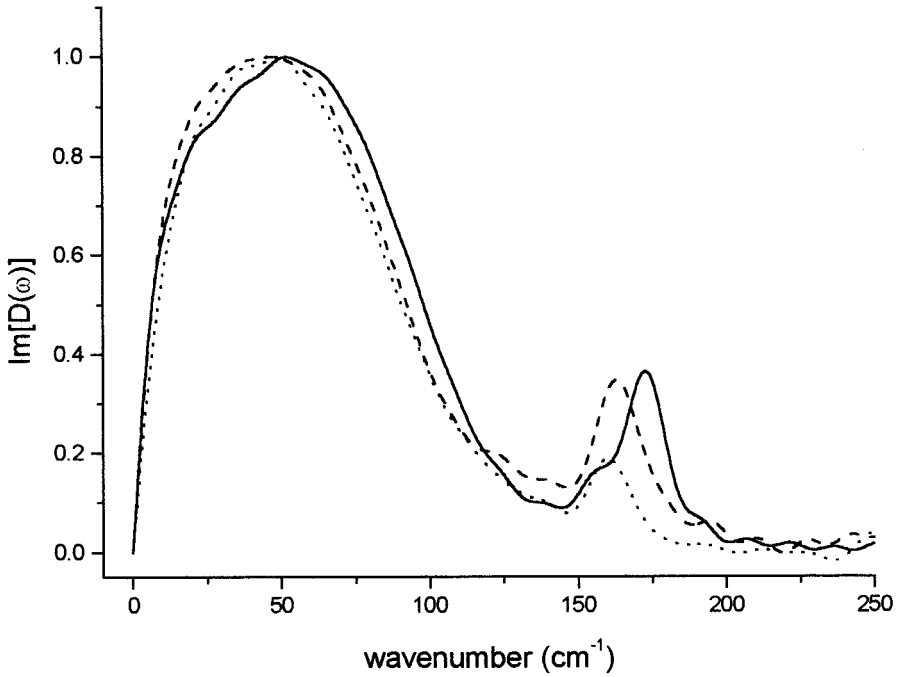

Figure 7. Spectral densities for BN (solid line) and its para methyl (dotted) and fluoro (dashed) derivatives. Data are presented in Table 2.

TABLE 2: Fitting Parameters to eq 2 + eq 3 for BN, *p*-Tolunitrile, and *p*-Fluorobenzonitrile[a]

	BN	*p*-tol	4-flu
b	0.09	0.06	0.08
ω_{BL} (cm^{-1})	14	13	11
α	1.00	1.00	1.00
g_1	0.91	0.94	0.92
ω_1 (cm^{-1})	61	46	45
$\Delta\omega$ (cm^{-1})	79	91	94
I_{eff} (amu Å^2)	184	281	285
$\omega_{1,BN}/\omega_1$	1	1.33	1.35
$(I/I_{BN})^{-1/2}$	1	1.23	1.24

[a] The frequencies of the Gaussian (eq 3) are compared with the predictions of the librational model (see text).

TABLE 3: Parameters Used in the Calculation of Diffusion Coefficients[a]

	a[a]/ Å	V[b]/ Å^3	ρ[c]	λ_1	λ_2	λ_3[d]	α_{xx}	α_{yy}	α_{zz}
BN	4.26	101	0.42	1.28	3.18	0.48			
NB	4.47	106	0.39	1.17	3.36	0.59	13.2	7.8	17.8

[a] The long semi-axis of the molecule. The width and thickness of the molecules were take to be the same for BN and NB, and equal to 3.2 and 1.77 Å, respectively. [b] The molecular volumes are calculated from the data given by Bondi (ref 88). [c] The axial ratio. [d] Taken from a linear interpolation of the data given in ref 81.

knowledge of the viscosity of the medium, η, the molecular volume, V, and the shape of the molecule. The shape dependence is expressed in λ_i, a numerical coefficient calculated by Youngren and Acrivos,[80] and presented in a modified form by Sension and Hochstrasser,[81] for an ellipsoid with three distinct axes. Thus all parameters in eqs 5 can be calculated and compared with experiment. This is done presently, and some of the data required for the calculations are presented in Table 3.

Initially we must address the issue that the τ_{r1} calculated according to the hydrodynamic model, eqs 5, are not the same as those measured in OHD−OKE, eq 1. The OHD−OKE experiment, and its frequency domain analogue, DLS, measure collective reorientation times, τ_{ci}, rather than the single molecule reorientation assumed in the hydrodynamic model.[51,52,79] To investigate the significance of this it is useful at first to approximate the shape of each of the monosubstituted benzenes studied here as an ellipsoid with two equal axes, in which case there are only two diffusion coefficients to be considered, $\Theta_\perp = \Theta_{xx} = \Theta_{yy}$, and $\Theta_{||} = \Theta_{zz}$. Then the slower relaxation time of eq 5 reduces to

$$\tau_{r1} = \frac{1}{6\Theta_\perp} = \frac{V_{eff}\eta}{kT} + \tau_r^0 \qquad (7)$$

where V_{eff} is the effective volume and the τ_r^0 is introduced empirically to account for the residual relaxation time as the viscosity approaches zero, which is expected to be close to the free rotor time of the molecule (but often is not, and is sometimes negative).[79] The effective volume is related to the molecular volume, V, by two numerical factors, one of which depends on the axial ratio of the ellipsoid and the other on whether a stick or slip boundary condition is assumed.[79,82,83] The collective relaxation time measured in the OHD−OKE experiment is related to τ_{r1} according to[51,52]

$$\tau_{c1} = \frac{g_2}{j_2}\tau_{r1} \qquad (8)$$

The factor g_2 is a measure of the static orientational correlations between pairs of molecules and takes the value of unity in the absence of such correlation. The factor j_2 accounts for dynamic angular momentum correlations between different molecules. Several experiments and some theoretical arguments suggest that in general $j_2 = 1 \pm 0.1$,[79] and this approximation is adopted here. In contrast g_2 has been reported to take values between 0.5 and 2.8 for NB,[51,79,84] while for BN the reported values vary between 1 and 1.55.[84,85] Clearly some further study of g_2 is required, and the OHD−OKE technique may be suitable, because of its wide dynamics range.

In Figure 8a the measurements of τ_{c1} for NB as a function of both temperature and dilution in an "inert" solvent are plotted against η/T, the numerical data being included in Table 1. The linear relationship suggests that the hydrodynamic model is

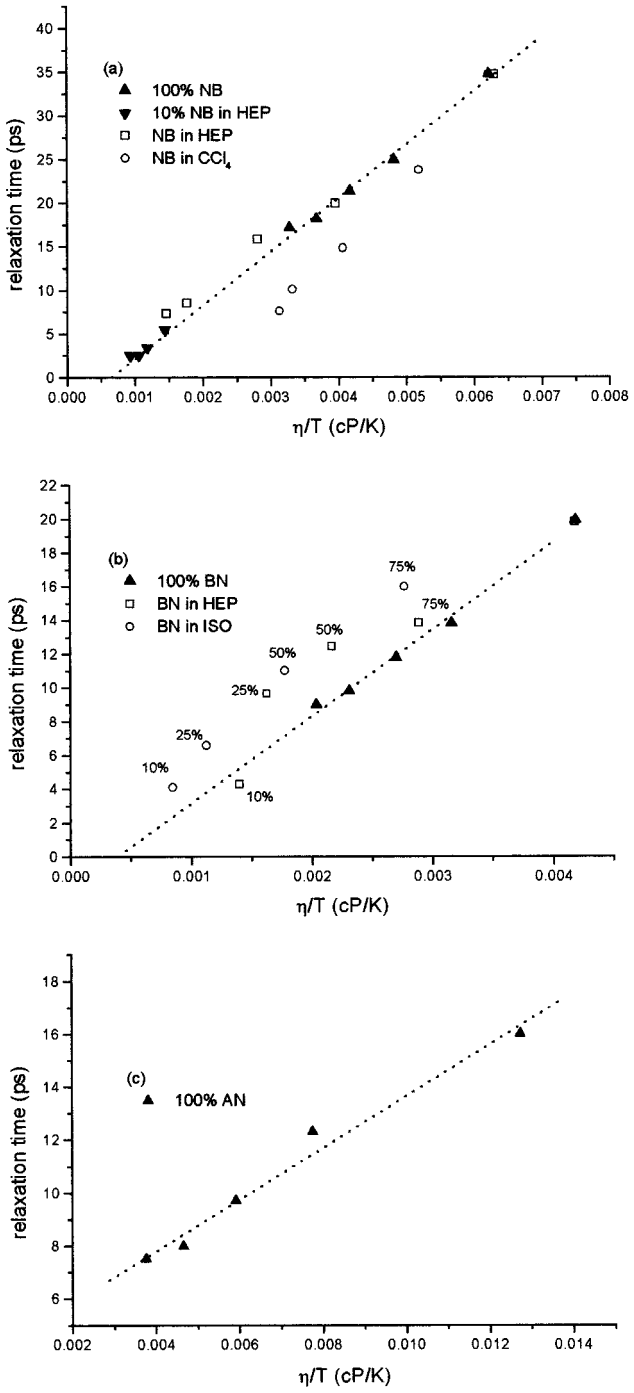

Figure 8. (a) Plot of the slowest relaxation time measured for NB as a function of η/T. Temperature dependent data are shown as filled symbols (▲ for neat NB, ▼ for a 10% volume fraction in heptane). Data at different dilution at 297 K are shown as open symbols (□ for dilution in heptane, ○ for CCl_4). (b) The same plot for BN. Temperature dependence of the neat liquid, ▲, dilution in heptane at 297 K, □, dilution in isopentane at 297 K, ○). (c) The same plot for AN, but only temperature dependent data of the neat liquid were recorded.

appropriate under these conditions. The temperature dependent measurements were made on neat NB and on a 10% solution of NB in heptane. By dissolving the solute in an inert solvent (heptane makes a negligible contribution to $R(t)$) it is expected that orientational correlations between molecules will be disrupted such that, at infinite dilution, $\tau_{c1} = \tau_{r1}$. From inspection of Figure 8a it is apparent that the extrapolation of the temperature dependent neat liquid data runs neatly through the temperature dependent solution data, which suggests $g_2 \approx 1$. The data for different dilutions of NB in heptane also lay close to the temperature dependent line, again consistent with $g_2 \approx 1$. When CCl_4 is the solvent a steeper slope is observed (Figure 8a) and τ_r^0 is rather strongly negative. Excluding the CCl_4 data (see below) all other measurements are consistent with a value of $g_2 = 1 \pm 0.1$. In Figure 8b the data for BN are shown, measured as a function of temperature for the neat liquid and dilution in isopentane and heptane. As for NB, the plot is linear and there is no remarkable deviation between the solution data and that for the neat solvent (excluding the CCl_4 data, not shown, which are again anomalous). This is consistent with a hydrodynamic model for the orientational relaxation, and with negligible static orientational correlations, $g_2 \approx 1$.

Two possibilities could result in the observed absence of static orientational pair correlations in NB and BN (AN was not studied, as it was only soluble in CCl_4, which gave inconsistent results). If molecular shape is crucial then the result is not a surprising one, since the substituted benzenes are not very anisotropic, compared to biphenyl, for example, where $g_2 = 1$ was also found.[64] On the other hand, if, as has been suggested,[84] electrostatic interactions are important then the large dipole moments of both of these molecules (4.2 D for NB and 4.4 D for BN[86]) might lead one to predict some orientational correlation. If the dipole−dipole interaction imposes any local structure it would appear from the present data to be short lived compared to the reorientation time, and so does not contribute to g_2. Alternatively, it is conceivable that local structure imposed by long-range intermolecular interactions does exist in the pure liquids, but the structure is oscillatory, leading to an average value of g_2 which is close to unity.[79]

The anomalous data for CCl_4 suggest that this is not a suitable "inert" solvent for the liquids studied here. Essentially the relaxation times observed in CCl_4 (which are in reasonable agreement with the DLS data of Alms et al.[51]) were always faster than predicted by the hydrodynamic model, leading to a large and negative τ_r^0. The reason for this is unclear at present, but we note that anomalous behavior has been reported when thiophene was diluted in CCl_4, an effect which was ascribed to solvent−solute complex formation.[28] A similar effect could be operating in these liquids, where the orientational dynamics are influenced by the formation and dissociation dynamics of the weak intermolecular complex on the picosecond time scale.

Turning now to the numerical analysis of the plots shown in Figures 8a and b we find from the slope and intercept, using eqs 6 and 7, that $V_{eff} = 85 \pm 7$ Å^3, $\tau_r^0 = -3.6$ ps for NB and $V_{eff} = 71 \pm 6$ Å^3, $\tau_r^0 = -2.0$ ps for BN. Temperature dependent, though not dilution, data have also been recorded for AN. These also behave hydrodynamically and lead (assuming $g_2 = 1$) to $V_{eff} = 13 \pm 3$ Å^3, $\tau_r^0 = 4.0$ ps (Figure 8c). The NB and BN data were extracted from the temperature dependent results alone. Including the data in alkane solvents leads to the similar volumes, but with larger errors. The V_{eff} for AN is anomalously low. The faster than expected reorientation time of AN has been noted previously[26] and will be discussed separately below. In the following paragraphs the focus will be on the analysis of the NB and BN data.

The small negative values of τ_r^0 are not surprising. They could arise from a calibration error in our measurements, but where there is overlap our data are in good agreement with literature values (e.g., for neat BN[24,33]). More likely the linear extrapolation from moderately high viscosity is of limited value. It is unlikely that the hydrodynamic model, which rests on the assumption of numerous collisions contributing small angle rotations, will be applicable as the viscosity approaches zero.

To interpret the experimental values of V_{eff} requires some assumptions on both the hydrodynamic boundary conditions and the molecular volume and shape. Studies of a wide range of liquids by DLS suggested that slip boundary conditions are appropriate for non H-bonding liquids.[87] Equation 7 already assumes two equal axes for the ellipsoid. The axial ratios, taken from the long axis of the molecules and the *thickness* of a benzene ring (1.77 Å), are given in Table 3, as are the molecular volumes, calculated according to the data given by Bondi.[88] Using these data and $\Theta_\perp = kT/\eta\lambda_\perp V$, where $\lambda_\perp$ is taken from ref 81, values of V_{eff} may be calculated. For NB we find 80.6 Å^3 and for BN 64 Å^3. These values are close to but somewhat lower than measured from the slopes of Figures 8a and b. This small difference might indicate that the slip boundary condition is not completely appropriate for NB and BN, but application of the stick boundary condition does not improve matters as it leads to a considerable overestimation of V_{eff}. (The ratio of slip to stick friction coefficients is 0.36 for $\rho = 0.4$.[82]) In addition to the numerical disagreement between experimental and calculated V_{eff} there are two points of ambiguity in this analysis. First, the choice of axial ratio, which gave reasonable agreement with the experimental data, was based on the *thickness* of the aromatic ring. However, there seems no reason not to choose the width, which leads to a much larger deviation between measured and calculated V_{eff}. In addition, if a slip boundary condition is retained then $\Theta_{||}$ becomes infinite and the second exponential, which is clearly present (Figure 1), disappears.

For these reasons it is necessary to attempt to analyze data in terms of an ellipsoid with three unequal axes, employing eqs 5 and 6, where the λ_i have been tabulated in ref 81. The results are presented in Figures 9a and 9b for NB and BN. In the sense of predicting a second exponential component, this more general analysis is an improvement on the symmetric rotor model. However, it is also clear from the figures that this is its only advantage. The disagreement between the longest experimentally measured and the calculated relaxation time is in fact larger than in the case of a symmetric ellipsoid, the calculated V_{eff} for BN being 32 Å^3 (based on the longest relaxation time) which is less than half the measured value.

On the basis of these data it must be concluded that the experimentally determined longest relaxation time measured for BN and NB is longer than predicted by hydrodynamic models with the slip boundary condition. Neither the imposition of a stick boundary condition nor taking account of three distinct molecular axes provides quantitative agreement between theory and experiment.

An additional factor that may account for the observation of a reorientation slower than predicted by hydrodynamics is the operation of dielectric friction. When a dipolar molecule in a polar medium reorients, it creates an electric field, which exerts a torque opposed to the reorientational motion. A model to account for this additional slowing down of orientational relaxation was developed by Nee and Zwanzig (NZ).[89] The NZ theory has since been applied many times, particularly to the case of orientational relaxation of a large dipolar dye molecule in solution.[90] Since the NZ theory is based on a dielectric continuum model of the medium, it is perhaps best suited to the case of large solute molecules in solvents of small diameter. However, it seems likely that similar dielectric friction effects will also operate for orientational relaxation in pure dipolar liquids, such as BN and NB, although more complex molecular treatments might be more appropriate.[91] However, an estimate of the significance of the dielectric friction contribution, τ_{DF}, to the total orientational relaxation time, τ_{OR}, of BN and NB

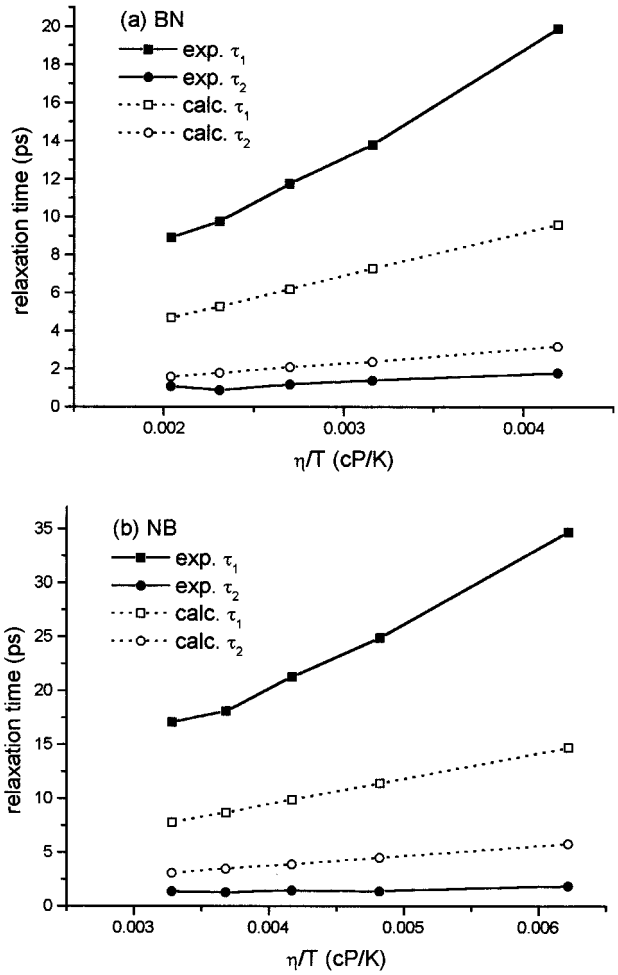

Figure 9. Plots of the two relaxation times extracted from the fit to eq 1 (solid lines) compared with the prediction of eqs 5 and 6 (dotted lines). (a) BN, (b) NB.

can be obtained by applying the NZ theory, in the form appropriate for polarizable liquids presented by Maroncelli[92]

$$\tau_{DF} = \frac{\xi_{DF}}{6kT} \tag{9}$$

where the dielectric friction term ξ_{DF} is given by

$$\xi_{DF} = \frac{2\mu^2}{a^3} f(\epsilon_r, n^2)\tau_D \tag{10}$$

in which μ is the dipole moment, a is a cavity radius, τ_D is the Debye dielectric relaxation time of the liquid, and

$$f(\epsilon, n^2) = \frac{(n^2+2)^2(\epsilon_r - n^2)}{3(2\epsilon_r + n^2)^2} \tag{11}$$

where n is the refractive index and ϵ_r the relative dielectric constant. In the case of BN at 297 K we calculate that $\tau_{DF} =$ 4.9 ps ($a = 3$ Å, $\mu = 4.2$ D, $\tau_D = 38$ ps, $\epsilon_r = 25$, $n^2 = 2.3$). This gives a total orientational relaxation time, $\tau_{OR} = \tau_{r1} + \tau_{DF}$, of 14.5 ps. This is closer to the experimental value of 20 ps. Thus the widely applied dielectric friction model may help to explain the difference between the relaxation time predicted by hydrodynamic models and the experimental data in the pure solvent. However, the fact that a linear relation between relaxation time and η/T is maintained independent of whether

the viscosity is altered by temperature or dilution in a nonpolar solvent (Figure 8) seems at odds with the explanation of the discrepancy through dielectric friction.

In summary the longest relaxation time determined in the OHD−OKE experiment is underestimated by conventional hydrodynamic models of orientational relaxation, even though the linear viscosity dependence predicted by the hydrodynamic model is observed. The inclusion of dielectric friction improves matters in the sense of providing a source of slowing the relaxation time, but it is not clear that this is the real reason for the disagreement between predicted and measured data. Rather, it is suggested that a combination of features that are not properly accounted for in the hydrodynamic theory contribute to the lack of a quantitative agreement between theory and experiment. First, it has been seen that the choice of the shape of the molecule alters considerably the calculated relaxation time. In particular it was found that the choice of two or three unequal axes to the ellipsoid altered the results. There are in general many difficulties in approximating the shape of these monosubstituted benzenes, which lack inversion centers, as ellipsoids of any kind, and this may contribute to the lack of agreement with the simplified hydrodynamic theory. In addition the slip boundary condition has been assumed throughout, in line with earlier studies of rotational diffusion of small molecules.[87] The imposition of stick boundary conditions makes the calculated relaxation times too long. However, it is possible that for polar polarizable molecules such as BN and NB some intermediate boundary condition might be more appropriate. There have been some earlier suggestions that slip boundary conditions are inappropriate for these polar molecules.[84]

This still leaves the problem of the origin of the fast relaxation time which has been observed here (and elsewhere[12,24,26,33]) for NB, BN, and AN, with a similarly fast exponential component being observed in OHD−OKE studies of a number of other liquids.[24,32,40,62,63] It is clear that the hydrodynamic model, which underestimates the slow relaxation time considerably, *overestimates* the fast relaxation time (Figure 9). Any additional contribution to the slow relaxation time, e.g., from dielectric friction, would presumably also act to slow the fast relaxation time as well. In addition it is noted that the experimentally determined pre-exponent values for the fast relaxation time are uniformly greater than those of the slower one, for example for NB at 297 K $A_1/A_2 = 1.6$. In contrast for NB we calculate, from eq 5 and Table 3, that the expected $A_1/A_2 = 0.43$. Finally, although when viewed in Figure 9 the fastest relaxation times appear to behave hydrodynamically, the temperature dependence is in fact rather weak (Table 1). For both NB and BN the decrease in lifetime is only slightly greater than the experimental error. Since neither the magnitude, weight, nor temperature dependence of the short lifetime are consistent with the theory, there seems no pressing reason to assign it to diffusive orientational relaxation. Bartolini et al. and, very recently, Loughnane et al. reached similar conclusions in their studies of iodobenzene[40] and a range of small molecules,[63] respectively.

This leaves the question of the origin of this fast exponential component. That its value is rather weakly dependent on temperature, compared to that of the longest relaxation time, was noted above. This recalls the behavior of the ultrafast spectral density (Table 1, Figure 5) and suggests that the short component is more sensitive to local intermolecular interactions than the bulk liquid viscosity. In contrast to the temperature dependence, the short relaxation time is sensitive to dilution to about the same extent as the longer relaxation time (the short component is not well resolved at high dilution). A stronger dependence on dilution than on the viscosity of the neat liquid might again suggest that intermolecular interactions are important in determining the magnitude of this component. It is difficult to assign a more detailed physical origin to this apparently nondiffusive picosecond component. One possibility is that it represents the dissociation or disruption of short-range structure in the liquid. It was noted earlier that there was no evidence for static orientational pair correlation between the dipolar molecules BN and NB ($g_2 \approx 1$). It is possible that electrostatic interactions between these polar and polarizable molecules do lead to local structures being formed in the liquid, but that they decay on the time scale of a few picoseconds, too rapidly to influence diffusive reorientation. In this case the fast picosecond component may be assigned to the disruption of such local structures in the liquid. Greenfield et al. proposed a similar model to account for their observations of a nonhydrodynamic picosecond component in the polarizability anisotropy relaxation of ethyl naphthalene.[94] Another possibility is that the interaction induced contributions to the polarizability anisotropy relaxation (or their cross term with orientational motion) in fact persist on the picosecond time scale and contribute the observed nondiffusive picosecond component in the OHD−OKE measurement; there is some evidence for such a long-lived contribution to the polarizability anisotropy relaxation from MD simulations.[49,72] Finally, it was noted very recently by Loughnane et al. that the fastest exponential relaxation times of a range of liquids correlated with the measured longest relaxation time. This result was discussed in terms of the short lifetime arising from spectral diffusion, which itself arises through molecular reorientational motion.[63] The correlation noted by Loughnane et al. is also found in our BN data, but it is less evident for NB.

This part of the discussion will close with some observations on the implications of the above result, that the fastest picosecond relaxation time appears nondiffusive in origin, for the time scale separation introduced into the analysis (section 2). In principle it would have been possible to analyze the entire spectral density, both the ultrafast and the slow "diffusive" parts, in terms of a series of BOs. The high frequency "ultrafast" part of the spectral density can be fit (imperfectly − Figure 4) with two underdamped or critically damped BOs, with $\gamma \leq \omega$ (Table 1). The fast picosecond component, now seen to be nondiffusive in origin, can be fit to an overdamped BO, $\gamma > \omega$, including the rising part (eq 1). For example, for neat BN we obtain an excellent fit to the data for the fastest component of eq 1 when it is transformed to the frequency domain and fit to eq 4 with the parameters, $\gamma = 140$ cm^{-1} and $\omega = 20$ cm^{-1} (Figure 10). Finally the long exponential component in the time domain, which can be approximately analyzed in terms of a diffusive exponential relaxation, can also be fit to a Lorentzian line shape in the frequency domain. The Lorentzian is the limiting form of an overdamped BO, $\gamma \gg \omega$. A similar hierarchy of under-, critically-, and overdamped oscillators was proposed by McMorrow and Lotshaw in their OHD−OKE study of the dynamics of liquid CS_2.[18] The advantage of analyzing the OHD−OKE data in terms of a series of BOs is that the rather artificial separation between diffusive and nondiffusive dynamics is not necessary. Indeed in the case of the fastest exponential component recovered from eq 1 such a separation now seems undesirable, and this component is best included with the "ultrafast spectral density". The disadvantage of the series of BOs approach is that the (unmodified) BOs do not provide an accurate fit to the high frequency line shape of these complex liquids. A second consequence of a nondiffusive origin of the fastest picosecond relaxation time is that BN and NB appear to reorient

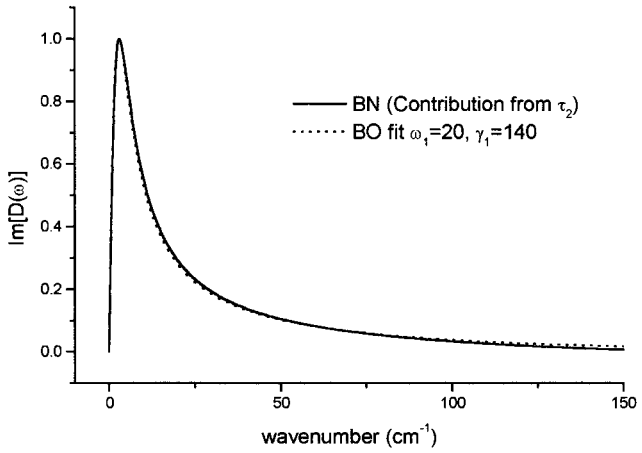

Figure 10. The fastest component of eq 1 (solid line) measured for BN, transformed to the frequency domain and fit to a single Brownian oscillator (dashed line).

as symmetric diffusers (angle exponential). This model also gave the best agreement between calculated and measured V_{eff}. However, the above noted ambiguity over the choice of axial ratio remains.

Finally we will close this section with some remarks on the temperature dependence of the slowest relaxation time of AN. The relaxation time at 297 K is the fastest of all the liquids studied here, although AN is by some way the most viscous liquid. We have commented earlier on the anomalous fast relaxation time of AN, in comparison to its (less viscous) methylated derivatives.[26] This result is not an artifact of the polarizability anisotropy relaxation measurement, because a similar trend is observed in dielectric relaxation and solvation dynamics experiments.[95,96] The new result here is that the relaxation time of AN appears to behave hydrodynamically, from the linear form of the plot in Figure 8c. However, the effective volume is too small (13 ± 3 Å^3), particularly when it is expected that, because of its ability to form H-bonds, AN is the liquid most likely to reorient under stick boundary conditions (as was observed for AN in alcohol solvents[97]). Previously we ascribed the anomalously fast relaxation time of AN to the dissociation of H-bonded structures in the liquid,[26] which may lead to faster than diffusive reorientation times.[98] In this case it is expected that the temperature dependence reflects activated H-bond dissociation, rather than bulk viscosity. In fact a plot of the $\ln(1/\tau_1)$ against $1/T$ is linear for AN. The linear plot of Figure 8c may reflect the fact that the temperature dependence of the viscosity is also often an exponentially activated process.[99]

Conclusion

The dynamics of liquid AN, BN, and NB have been recorded as a function of temperature and dilution. The dynamics were measured with the good signal-to-noise and wide dynamic range characteristic of the OHD−OKE method.

The long time relaxation (>1 ps) is characterized by biexponential kinetics. Studies as a function of dilution and temperature of the longest of these relaxation times did not reveal any evidence for the existence of static orientational pair correlation in liquid BN or NB. Although this long relaxation time was found to behave hydrodynamically it was not possible to account quantitatively for the viscosity dependence, on the basis of simple models of molecular shape, using either stick or slip boundary conditions. It was suggested that either these hydrodynamic boundary conditions were inappropriate for these liquids, some intermediate boundary condition being required, or that the nonspheroidal shape of the molecules leads to a disagreement with the predictions of the hydrodynamic theory.

The shorter of the two exponential relaxation times decreased only slightly with increasing temperature but was more sensitive to dilution in a nonpolar solvent. This picosecond relaxation time, which is found in many benzene derivatives, was too fast to be ascribed to diffusive reorientation. It was suggested that this component arises from structural dynamics in the liquid, or possibly from interaction induced relaxation. The fact that this component cannot be ascribed to orientational diffusion puts a question mark over the commonly used separation of the spectral density into fast and slow diffusive contributions. An alternative description of the spectral density in terms of a series of increasingly damped Brownian oscillators was discussed.

The high frequency part of the spectral density, obtained from the OHD−OKE measurement by standard Fourier transform methods, was fit to two line shape functions − ohmic and antisymmetrized Gaussian. With these two functions the fit was always good. The dominant part of the response was the Gaussian term. Other functions which were used to fit the spectral densities were a dual Brownian oscillator and two antisymmetrized Gaussians. Both gave less good fits than the ohmic plus Gaussian analysis, the latter being unacceptable for the three liquids studied here. The dual BO fits were acceptable in many cases, but invariably failed to fit the high frequency part of the response, because the BO function only slowly returns to the baseline.

The dominant, Gaussian, part of the high frequency spectral density was ascribed to librational motion of molecules on a potential surface formed by interactions with a cage of their neighbors. Three derivatives of BN with different moments of inertia were studied, and the frequency shifts of the spectral densities were qualitatively consistent with this interpretation. The librational frequency is not expected to be a strong function of temperature, as was observed. On dilution of BN and NB in nonpolar solvents the ultrafast spectral densities shifted to lower frequency and narrowed. This was ascribed to the change in the force constant of the potential well created by the nearest neighbors when a polar and polarizable molecule was replaced by an alkane.

Acknowledgment. S.R.M. is grateful to EPSRC for generous equipment support. N.A.S. thanks the EPSRC for a research studentship.

References and Notes

(1) *Spectroscopy and Relaxation of Molecular Liquids*, Studies in Physical and Theoretical Chemistry; Steele, D., Yarwood, J., Eds.; Elsevier: Amsterdam, 1991; Vol. 74.

(2) *Collision- and Interaction- Induced Spectroscopy*; Tabisz, G. C., Neuman, M. N., Eds.; NATO ASI series C, Kluwer Academic: Dordrecht, 1995.

(3) Böttcher, C. J. F.; Bordewijk, P. *Theory of Electric Polarisation*; Elsevier: Amsterdam, 1973.

(4) Yarwood, J. *Annu. Rep. Prog. Chem., Section C* **1990**, *87*, 75 and earlier reviews by the same author in this series.

(5) Barbera, P. F.; Jarzeba, W. *Acc. Chem. Res.* **1988**, *21*, 195.

(6) Weaver, M. J.; McManis, G. E., III *Acc. Chem. Res.* **1990**, *23*, 294.

(7) Yoshihara, K.; Tominaga, K.; Nagasawa, Y. *Bull. Chem. Soc. Jpn.* **1995**, *68*, 696.

(8) Bixon, M.; Jortner, J. *Chem. Phys.* **1993**, *176*, 467.

(9) Rips, I.; Jortner, J. *J. Chem. Phys.* **1987**, *87*, 2090.

(10) Rips, I.; Jortner, J. *J. Chem. Phys.* **1987**, *87*, 6513.

(11) Zusman, L. D. *Chem. Phys.* **1988**, *119*, 51.

(12) Lotshaw, W. T.; McMorrow, D.; Kenney-Wallace, G. A. *Proc. SPIE* **1988**, *981*, 20.

(13) McMorrow, D.; Lotshaw, W. T. *J. Phys. Chem.* **1991**, *95*, 10395.

(14) Back, R.; Kenney-Wallace, G. A.; McMorrow, D.; Lotshaw, W. T. *Chem. Phys. Lett.* **1992**, *191*, 423.

(15) McMorrow, D.; Lotshaw, W. T. *Chem. Phys. Lett.* **1993**, *201*, 369.

(16) McMorrow, D.; Lotshaw, W. T. *Chem. Phys. Lett.* **1990**, *174*, 85.
(17) McMorrow, D.; Lotshaw, W. T. *IEEE J. Quantum Electron.* **1988**, *24*, 443.
(18) McMorrow, D.; Lotshaw, W. T. *Chem. Phys. Lett.* **1991**, *178*, 69.
(19) Palese, S.; Mukamel, S.; Miller, R. J. D.; Lotshaw, W. T. *J. Phys. Chem.* **1996**, *100*, 10380.
(20) McMorrow, D.; Thantu, N.; Melinger, J. S.; Kim, S. K.; Lotshaw, W. T. *J. Phys. Chem.* **1996**, *100*, 10389.
(21) Chang, Y. J.; Castner, E. W., Jr. *J. Phys. Chem.* **1994**, *98*, 9712.
(22) Chang, Y. J.; Castner, E. W., Jr. *J. Chem. Phys.* **1993**, *99*, 113.
(23) Chang, Y. J.; Castner, E. W., Jr. *J. Chem. Phys.* **1993**, *99*, 7289.
(24) Chang, Y. J.; Castner, E. W., Jr. *J. Phys. Chem.* **1996**, *100*, 3330.
(25) Smith, N. A.; Lin, S.; Meech, S. R.; Shirota, H.; Yoshihara, K. *J. Phys. Chem. A* **1997**, *101*, 9578.
(26) Smith, N. A.; Lin, S.; Meech, S. R.; Yoshihara, K. *J. Phys. Chem. A* **1997**, *101*, 3641.
(27) Shirota, H.; Yoshihara, K.; Smith, N. A.; Lin, S.; Meech, S. R. *Chem. Phys. Lett.* **1997**, *281*, 27.
(28) Kamada, K.; Ueda, M.; Sakaguchi, T.; Ohta, K.; Fukumi, T. *Chem. Phys. Lett.* **1996**, *249*, 329.
(29) Kamada, K.; Ueda, M.; Ohta, K.; Wang, Y.; Ushida, K.; Tominaga, Y. *J. Chem. Phys.* **1998**, *109*, 10948.
(30) Quitevis, E. L.; Neelakandan, M. *J. Phys. Chem.* **1996**, *100*, 10005.
(31) Neelakandan, M.; Pant, D.; Quitevis, E. L. *Chem. Phys. Lett.* **1997**, *265*, 283.
(32) Neelakandan, M.; Pant, D.; Quitevis, E. L. *J. Phys. Chem. A* **1997**, *101*, 2936.
(33) Cong, P.; Deuel, H. P.; Simon, J. D. *Chem. Phys. Lett.* **1995**, *240*, 72.
(34) Cong, P.; Simon, J. D.; She, C. Y. *J. Chem. Phys.* **1996**, *104*, 962.
(35) Wynne, K.; Galli, C.; Hochstrasser, R. M. *Chem. Phys. Lett.* **1992**, *193*, 17.
(36) Kinoshita, S.; Kai, Y.; Yamaguchi, M.; Yagi, T. *Phys. Rev. Lett.* **1995**, *75*, 148.
(37) Kinoshita, S.; Kai, Y.; Yamaguchi, M.; Yagi, T. *Chem. Phys. Lett.*, **1995**, *236*, 259.
(38) Kinoshita, S.; Kai, Y.; Watanabe, Y. *Chem. Phys. Lett.* **1999**, *301*, 183.
(39) Steffen, T.; Meinders, N. A. C. M.; Duppen, K. *J. Phys. Chem. A* **1998**, *102*, 4213.
(40) Bartolini, P.; Ricci, M.; Torre, R.; Righini, R.; Sánta, I. *J. Chem. Phys.* **1999**, *110*, 8653.
(41) Cho, M.; Du, M.; Scherer, N. F.; Fleming, G. R.; Mukamel, S. *J. Chem. Phys.* **1993**, *99*, 2410.
(42) Berne, B. J.; Pecora, R. *Dynamic Light Scattering* 1976, Wiley: New York.
(43) Maroncelli, M.; Kumar, V. P.; Papazyan, A. *J. Phys. Chem.* **1993**, *97*, 1.
(44) Cho, M.; Rosenthal, S. J.; Scherer, N. F.; Ziegler, L. D.; Fleming, G. R. *J. Chem. Phys.* **1992**, *96*, 5033.
(45) Rainieri, F. O.; Friedman, H. L. *J. Chem. Phys.* **1994**, *101*, 6111.
(46) Stratt, R. M.; Maroncelli, M. *J. Phys. Chem.* **1996**, *100*, 12981.
(47) Ladanyi, B. M. In *Electron and Ion Transfer in Condensed Matter*; Eds. Kornyshev, A. A., Ulstrup, J. World Scientific: Singapore, 1997.
(48) Ladanyi, B. M.; Stratt, R. M. *J. Phys. Chem.* **1995**, *99*, 2502.
(49) Ladanyi, B. M.; Liang, Y. Q. *J. Chem. Phys.* **1995**, *103*, 6325.
(50) Bucaro, J. A.; Litovitz, T. A. *J. Chem. Phys.* **1971**, *54*, 3846.
(51) Alms, G. R.; Bauer, D. R.; Brauman, J. I.; Pecora, R. *J. Chem. Phys.* **1973**, *59*, 5310.
(52) Keyes, T.; Kivelson, D. *J. Chem. Phys.* **1974**, *56*, 1057.
(53) Smith, N. A.; Meech, S. R. *Faraday Trans.* **1997**, *108*, 35.
(54) Maroncelli, M.; Castner, E. W., Jr. *J. Mol. Liq.* **1998**, *77*, 1.
(55) Tanimura, Y.; Mukamel, S. *J. Chem. Phys.*, **1993**, *99*, 9496.
(56) Tominaga, K.; Yoshihara, K. *Phys. Rev. Lett.* **1995**, *74*, 3061.
(57) Tominaga, K.; Yoshihara, K. *J. Chem. Phys.* **1996**, *104*, 1159.
(58) Steffen, T.; Duppen, K. *Phys. Rev. Lett.* **1996**, *76*, 1224.
(59) Tokamakoff, A.; Fleming, G. R. *J. Chem. Phys.* **1997**, *106*, 2569.
(60) Ruhman, S.; Kohler, B.; Joly, A. G.; Nelaon, K. A. *Chem. Phys. Lett.*, **1987**, *141*, 16.
(61) Ruhman, S.; Nelson, K. A. *J. Chem. Phys.* **1991**, *94*, 859.
(62) Farrar, R. A.; Loughnane, B. J.; Deschenes, L. A.; Fourkas, J. T. *J. Chem. Phys.* **1997**, *106*, 6901.
(63) Loughnane, B. J.; Scodinu, A.; Farrar, R. A.; Fourkas, J. T. *J. Chem. Phys.* **1999**, *111*, 2686.
(64) Deeg, F. W.; Stankus, J. J.; Greenfield, S. R.; Newell, V. J.; Fayer, M. D. *J. Chem. Phys.* **1989**, *90*, 6893.
(65) For a recent review of the theoretical background to OHD−OKE see Kinoshita, S.; Kai, Y.; Ariyoshi, T.; Shimada, Y. *Int. J. Mod. Phys. B*, **1996**, *10*, 1229.
(66) Leggett, A. J.; Chakravarty, S.; Dorsey, A. T.; Fisher, M. P. A.; Garg, A.; Zwerger, W. *Rev. Mod. Phys.* **1987**, *59*, 1.
(67) Tanimura, Y.; Mukamel, S. In *Femtosecond Reaction Dynamics*; Wiersma, D. A., Ed.; Elsevier: North Holland, Amsterdam, 1994.
(68) Friedman, J. S.; She, C. Y. *J. Chem. Phys.* **1993**, *99*, 4960.
(69) *CRC Handbook of Chemistry and Physics, 58th Edition*, CRC Press: Boca Raton, FL, 1977.
(70) Lotshaw, W. T.; Staver, P. R.; McMorrow, D.; Thantu, N.; Melinger, J. S. In *Ultrafast Phenomena IX*; Barbar, P. F., Knox, W., Mourou, G. A., Zewail, A. H., Eds.; Springer Series in Chemical Physics, **1994**, *60*, 91.
(71) Lynden-Bell, R. M.; Steele, W. A. *J. Phys. Chem.* **1984**, *88*, 6514.
(72) Ladanyi, B. M.; Klein, S. *J. Chem. Phys.* **1996**, *105*, 1552.
(73) Yeh, J. Y.; Shen. T.-L.; Nocera, D. G.; Leroi, G. E.; Suzuka, I.; Ozawa, H.; Namuta, Y. *J. Phys. Chem.* **1996**, *100*, 4385.
(74) Venturo, V. A.; Felker, P. M. *J. Chem. Phys.* **1993**, *99*, 748.
(75) Debye, P. in *'Polar Molecules'*, Dover: New York, 1928.
(76) Perrin, F. *J. Phys. Radium.* **1934**, *5*, 497.
(77) Dorfmüller, Th., Pecora, R., Eds., *'Rotational Dynamics of Small Molecules'*, Springer, Berlin, 1987.
(78) Steele, W. A. in ref 1, p63.
(79) Kivelson, D.; Madden, P. A. *Annu. Rev. Phys. Chem.* **1980**, *31*, 523.
(80) Youngren, G. K.; Acrivos, A. *J. Chem. Phys.* **1975**, *63*, 3846.
(81) Sension, R. J.; Hochstrasser, R. M. *J. Chem. Phys.* **1993**, *98*, 2490.
(82) Hu, C.-M.; Zwanzig, R. *J. Chem. Phys.* **1974**, *60*, 4354.
(83) Barkley, M. D.; Kowalczyk, A. A.; Brand, L. *J. Chem. Phys.* **1981**, *75*, 3581.
(84) Bertucci, S. J.; Burnham, A. K.; Alms, G. R.; Flygare, W. H. *J. Chem. Phys.* **1977**, *66*, 605.
(85) Whittenberg, S. L.; Wang, C. H. *J. Chem. Phys.* **1979**, *71*, 561.
(86) Smith, J. W. *Electric Dipole Moments;* |, Butterworth: London.
(87) Bauer, D. L.; Brauman, J. I.; Pecora, R. *J. Am. Chem. Soc.* **1974**, *96*, 6840.
(88) Bondi, A. *J. Phys. Chem.* **1964**, *68*, 441.
(89) Nee, T. W.; Zwanzig, R. *J. Chem. Phys.* **1970**, *52*, 6353.
(90) Laitinen, E.; Korppi-Tommola, J.; Linnanto, J. *J. Chem. Phys.* **1997**, *107*, 7601, and references therein.
(91) Madden, P.; Kivelson, D. *J. Phys. Chem.* **1982**, *86*, 4244.
(92) Maroncelli, M. *J. Chem. Phys.* **1997**, *106*, 1545.
(93) Landolt-Bornstein *Atom und Molekularphysik*; Springer-Verlag: Berlin, 1951; *1 (part3)*, p 511.
(94) Greenfield, S. R.; Sengupta, A.; Stankus, J. J.; Terazima, M.; Fayer, M. D. *J. Phys. Chem.* **1994**, *98*, 313.
(95) Garg, S. K.; Smyth, C. P. *J. Chem. Phys.* **1967**, *46*, 373.
(96) Pal, H.; Nagasawa, Y.; Tominaga, K.; Yoshihara, K. *J. Chem. Phys.* **1995**, *19*, 7758.
(97) Myers, A. B.; Pereira, M. A.; Holt, P. L.; Hochstrasser, R. M. *J. Chem. Phys.* **1987**, *86*, 5146.
(98) Matsumoto, M.; Gubbins, K. E. *J. Chem. Phys.* **1990**, *93*, 1981.
(99) Branin, F. H., Jr.; Smyth, C. P. *J. Chem. Phys.* **1952**, *20*, 1121.